한국소성가공학회 2003 년도 춘계학술대회 논문집 pp.465~469

변형 LIGA 공정을 이용한 마이크로 렌즈 어레이 개발: 몰딩 및 모델링

김동성* · 이현섭 · 양상식 · 이봉기 · 이성근 · 권태헌 · 이승섭

Formation of Microlens Array via a Modified LIGA Process: Molding and Modeling

D. S. Kim, H. S. Lee, S. S. Yang, B.-K. Lee, S.-K. Lee, T. H. Kwon and S. S. Lee

Abstract

Microlens arrays were fabricated using a novel fabrication technology based on the exposure of a PMMA (Polymethylmethacrylate) sheet to deep X-rays and subsequent thermal treatment. X-ray irradiation causes the decrease of molecular weight of PMMA, which in turn decreases the glass transition temperature and consequently causes a net volume increase during the thermal cycle resulting in a swollen microlens. A new physical modeling and analyses for microlens formation were presented according to experimental procedure. A simple analysis based on the new model is found to be capable of predicting the shapes of microlens which depend on the thermal treatment. For the replication of microlens arrays having various diameters with different foci on the same surface, the hot embossing and the microinjection molding processes has been successfully utilized with a mold insert that is fabricated by Ni-electroplating based on a PMMA microstructure of microlenses. Fabricated microlenses showed good surface roughness with the order of 1nm.

Key Words : Microlens array, Modified LIGA process, Glass transition temperature, Modeling, Analysis, Hot embossing and Microinjection molding

1. 서 론

Microlenses have emerged as essential components in optical communication, optical storage system, bio-medical instruments, and so on. There have been many methods of fabricating a microlens or a microlens array. Recently our group (Lee *et al.*) proposed a new modified LIGA process. According to the process, microlens array could be fabricated from PMMA sheets through the simple steps of a deep X-ray exposure and a thermal treatment, without development of the PMMA [1].

* 포항공과대학교 기계공학과

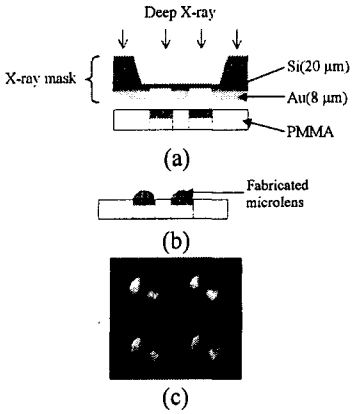

Fig. 1 Proposed fabrication process: (a) Step 1, X-ray irradiation, (b) Step 2, thermal treatment, and (c) fabricated microlenses by a modified LIGA process

Fig. 1 shows the schematic of the microlens fabrication process and fabricated microlenses. The fabrication process consists of two steps: (1) *X-ray irradiation*: a PMMA sheet gets exposed by deep X-ray with a certain dose as depicted in Fig. 1(a), (2) *thermal treatment*: the X-ray exposed PMMA is put into a furnace at a preset heating temperature. Then the PMMA sheet is cooled by air in room temperature (Fig. 1(b)). Finally we can obtain the micro-lens as shown in Fig. 1(c).

In this regard, we present a physical modeling with an analysis method and also present replication methods, hot embossing and microinjection molding, of microlens array fabricated by the proposed modified LIGA process.

2. 마이크로 렌즈 형성에 대한 모델링 및 해석 [2]

2.1 물리적 모델링

In a deep X-ray lithography, the molecular weight after the X-ray irradiation is characterized as below:

$$\frac{1}{M_w} = \frac{1}{M_{w0}} + \frac{(G_s - 4G_x)D}{200N_A} \tag{1}$$

where M_w, M_{w0}, D, G_s, G_x, N_A are molecular weight, initial molecular weight in [g/mol], X-ray dose in [J/cm^3], the amount of polymer chain scission, the number of cross-linking per 100eV of energy absorbed, and Avogadro's number, respectively.

In our experiments, the X-ray dose is well characterized by the following function of thickness h [μm]:

$$D(h) = 2.594\times10^{-10}h^4 - 1.416\times10^{-6}h^3 + 3.016\times10^{-3}h^2 - 3.385h + 2397.6 \tag{2}$$

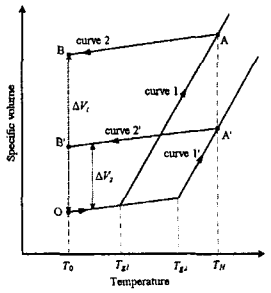

Fig. 2 Schematic of mechanism of microlens formation

With $M_{w0} = 0.9 \times 10^6$ g/mol, the G factor is obtained as a nonlinear function of the dose:

$$G(D) \equiv (G_s - 4G_x) = 200N_A \frac{0.0432}{M_{w0}}\left(1 - \frac{0.567}{D(h)^{0.5757}}\right)D(h)^{0.1514} \tag{3}$$

The decrease of M_w caused by X-ray exposure in turn causes the decrease of glass transition temperature, T_g.

$$T_g = T_{g,\infty} - \frac{K}{X_n} \tag{4}$$

where X_n is the number-averaged chain length, K is a polymer-specific constant and $T_{g,\infty}$ is the asymptotic value. In this case, values of $T_{g,\infty}$ and K are 384±1(K) and 1607±170(K), respectively.

The change of T_g in the thickness direction plays the key role of the lens formation. This mechanism of volume increase is as schematically shown in Fig. 2.

The net volume increase for a portion exposed by X-ray irradiation induced during a thermal cycle, i.e. from O to B (or B') as shown in Fig. 2, can be calculated by

$$\Delta V_{nr} = \int_{V_{exposed}} \Delta\alpha\left(T_H - T_g(h)\right)H\left(T_H - T_g(h)\right)dV - \int_{V_{exposed}} \Delta\alpha\left(T_H - T_{g,\infty}\right)H\left(T_H - T_{g,\infty}\right)dV \tag{5}$$

where ΔV_{nr} denotes the net volume increase without

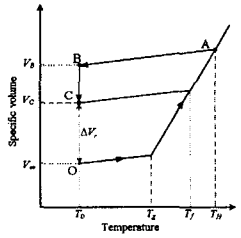

Fig. 3 Relaxation of free volume: relation between temperature and specific volume of polymer.

the volume relaxation phenomena. $\Delta\alpha$ denotes (α_r - α_g) where α_r and α_g are volumetric thermal expansion coefficients, 490×10^{-6} K^{-1} and 213×10^{-6} K^{-1}, in rubbery and glassy states, respectively. T_H denotes a heating temperature. $H(T)$ is heaviside step function.

The volume change during the thermal cycle of polymer having T_g is schematically shown in Fig. 3. The final net volume increase with the volume relaxation can be calculated by the following Equation:

$$\begin{aligned}\Delta V_r &= V_C - V_\infty = V_B - V_\infty + \left(\delta_V - \delta_V^0\right)V_\infty \\ &= \Delta V_{nr} + \Delta\delta_V V_\infty\end{aligned} \tag{6}$$

One can get the evolution equation for δ_V combining with the fictive temperature to represent the thermo-dynamically non-equilibrium state:

$$\Delta\delta_V(h) = \int_{t_{ci}}^{t_{cf}} \left\{ -\Delta\alpha \cdot \left[\frac{e}{\left(T_g(h) - T_{cool}(t)\right)\beta} + \sigma \right]^{-1} \right\} \cdot H\left(T_H - T_g(h)\right)\frac{dt}{t} \tag{7}$$

where e, β, σ, t_{ci}, t_{cf} and $T_{cool}(t)$, denote are the base of natural log, nonexponentiality, nonlinearity, the time when the cooling starts and ends in [min] and cooling temperature, respectively.

2.2 마이크로 렌즈 형상의 해석

The microlens shape was described by the second order polynomial based on augmented Young-Laplace equation. The maximum height of the microlens is to be determined combining with Equation (6) as follows:

i) when ΔV_{nr} is used:

$$\begin{aligned}y_{\max} = 2&\int_0^{h_{\max}} \Delta\alpha\left(T_H - T_g(h)\right)H\left(T_H - T_g(h)\right)dh \\ -2&\int_0^{h_{\max}} \Delta\alpha\left(T_H - T_{g,\infty}\right)H\left(T_H - T_{g,\infty}\right)dh\end{aligned} \tag{8}$$

where $y_{\max}$ and $h_{\max}$ mean maximum height of the microlens and the total thickness of the PMMA sheet.

ii) when ΔV_r is used:

$$\begin{aligned}y_{\max} = 2&\int_0^{h_{\max}} \left[\Delta\alpha\left(T_H - T_g(h)\right) + \Delta\delta_V(h)\right]H\left(T_H - T_g(h)\right)dh \\ -2&\int_0^{h_{\max}} \left[\Delta\alpha\left(T_H - T_{g,\infty}\right) + \Delta\delta_{V,plate}\right]H\left(T_H - T_{g,\infty}\right)dh\end{aligned} \tag{9}$$

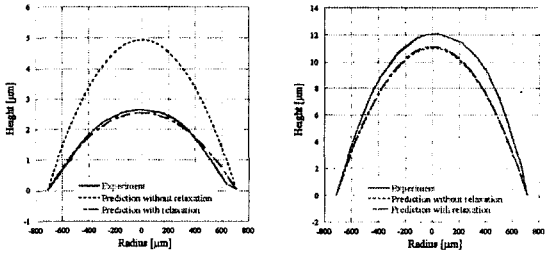

(a) T_H = 105°C (b) T_H = 115°C

Fig. 4 Predicted microlens shapes with experimental ones (solid) at two different heating temperatures of (a) 105°C (b) 115°C: predictions without considering the relaxation process (dotted), and with considering the relaxation process (broken).

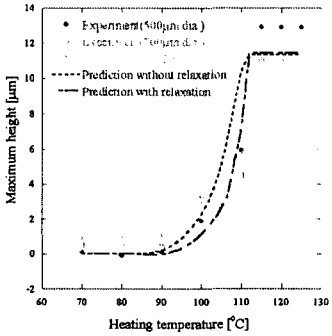

Fig. 5 Predicted maximum heights of microlenses as a function of heating temperature with experiments (solid), predictions without relaxation process (dotted) and with relaxation process (broken).

2.3 해석 결과

Fig. 4(a) and (b) show microlens shapes from the real experiments and the shapes for two heating temperature cases of 105°C and 115°C.

Plotted in Fig. 5 are variations of the maximum heights of microlens as a function of heating temperature obtained from the experiments (500μm, 700μm and 1000μm in diameters), as well as modeling and simulation results based on Equations (8) and (9) developed in this study.

3. 핫 엠보싱 [3]

In this study, using the microlens array, fabricated by the modified LIGA process, Ni-electroplating mold insert is fabricated. This master is composed of 500μm diameter array (2 × 2), 300μm diameter array (2 × 2), 200μm diameter array (5 × 5), 70μm diameter array (5 × 5) as shown in Fig. 6.

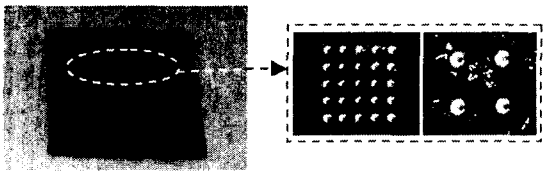

Fig. 6 Photographs of Ni-electroplated mold insert

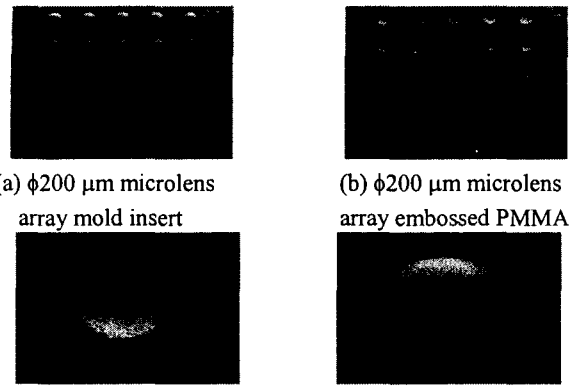

(a) ϕ200 μm microlens array mold insert

(b) ϕ200 μm microlens array embossed PMMA

(c) ϕ300 μm microlens mold insert

(d) ϕ300 μm microlens embossed PMMA

Fig. 7 SEM images to compare the surface roughness of the mold insert and the embossed PMMA.

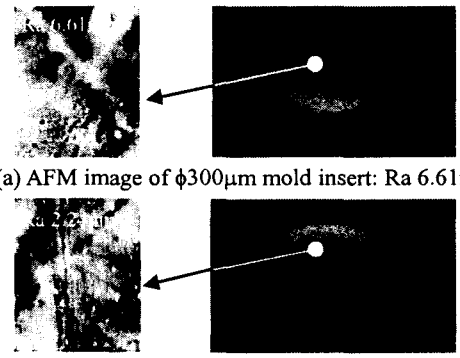

(a) AFM image of ϕ300μm mold insert: Ra 6.61nm

(b) AFM image of ϕ300μm embossed microlens: Ra 2.24nm

Fig. 8 AFM images to compare the surface roughness of mold insert and embossed PMMA.

Hot embossing experiments are performed with various processing conditions. Standard conditions are as follows: embossing temperature 130 °C, deembossing temperature 80 °C, holding time 5 min, and embossing velocity 10μm/s. The height difference between mold insert and embossed PMMA is about 0.6μm (4% of total mold insert height). The height difference might be caused by the entrapped air and/or the shrinkage of PMMA during cooling. The SEM images of mold insert together with duplicated microlens arrays are shown in Fig. 7. Fig. 7 shows that the surface roughness of the embossed PMMA is somehow better than that of mold insert. This fact is confirmed in Fig. 8 showing AFM (AutoProbe M5, PSIA Co.) scanning images of mold insert and embossed PMMA together with Ra (surface roughness) values. Master microlens array fabricated by the modified LIGA process has very good surface roughness (Ra 0.5nm), but the surface roughness of the electroplated mold insert becomes slightly coarse (Ra 6.61nm). However, the final embossed PMMA shows better surface roughness (Ra 2.24nm) than the mold insert. The reason for the improved surface roughness in the replicated microlens array is not clear at this moment, but might be due to the detachment from the mold insert surface and subsequent reflow during cooling.

4. 마이크로 사출성형 [4]

A conventional injection molding machine was used to replicate the electroplated Ni mold insert as shown in Fig. 6. The injection molding experiments were performed with three general polymeric materials (PS, PMMA and PC). These materials have different refractive indices (1.49~1.59), which will give the different optical properties of final products. Experiments were performed for seven processing conditions by changing filling time, packing pressure and packing time for each polymeric material.

The surface profiles of the molded microlenses (PC) for different packing pressures - 5, 10 and 15 MPa – are depicted in Fig.9 together with the surface profile of the mold insert. The heights of the replicated microlens arrays are a little smaller than those of the mold insert. We presume that the deviation results from the shrinkage of polymeric materials after the molding process. The results of Fig.9 imply that the optimal packing pressure may solve the shrinkage problem. *Ra* values of 300μm lenses and the mold insert were measured with an AFM (Bioscope AFM, Digital Instruments). Molded microlenses have smaller *Ra* than the mold insert.

Fig.10 shows a measured birefringence distribution of the molded product (PMMA). The small surface roughness and birefringence of the molded microlenses indicate a possibility of using the microlens arrays for optical applications.

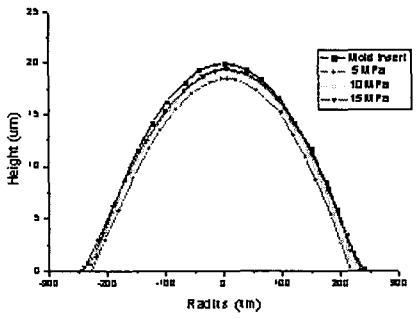

Fig. 9 Surface profiles of the injection molded ϕ 500μm micro-lenses (PC) with mold insert.

Fig. 10 Birefringence distribution of molded PMMA

5. 결론

In this study, we have presented a simple microlens

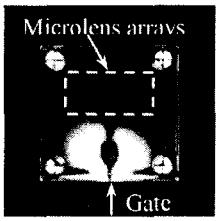

fabrication consisted of X-ray irradiation and the following thermal treatment. A physical modeling and an analysis tool also developed to predict the shape of microlens formation during the thermal cycle of the deep X-ray exposed PMMA sheet, based on fundamental polymer physics with the free volume theory including the volume relaxation phenomena. Replications of microlens arrays were successfully performed based on hot embossing and microinjection molding processes with good surface roughness.

Proper characterization of glass transition temperature decrease caused by molecular weight decrease of PMMA exposed to X-ray irradiation was suggested. The physical modeling of free volume increase during the thermal cycle and subsequent volume relaxation was also presented. For an analysis of microlens formation, based on the augmented Young-Laplace equation, the second order polynomial was chosen to describe the cross-sectional shape of swollen microlens with a surface tension taken into account. The prediction model could be eventually used in determining the detailed thermal treatment conditions for a desired microlens shape with a specific focal length fabricated by the modified LIGA process.

The heights of hot embossed and microinjection molded microlenses were slightly smaller than the mold insert and the surface roughness of molded microlenses was better than that of mold insert.

The molded microlens arrays could be applied to various optical applications that need microlens arrays which have the different foci on the same surface.

후 기

The authors would like to thank Korean Ministry of Science and Technology for the financial supports via the National Research Laboratory Program (2000-N-NL-01-C-148).

참 고 문 헌

(1) S.-K. Lee, K.-C. Lee and S. S. Lee, 2002, "A Simple Method for Microlens Fabrication by the Modified LIGA Process", J. Micromech. Microeng., Vol. 12, pp. 334~340.

(2) D.S. Kim, S.S. Yang, S.-K. Lee, T.H. Kwon and S.S. Lee, 2002, "Physical Modeling and Analysis of Microlens Formation Fabricated by a Modified LIGA Process", J. Micromech. Microeng., in press.

(3) H.S. Lee, S.-K. Lee, T.H. Kwon and S.S. Lee, "Microlenses array Fabrication by Hot embossing process", Optical MEMS 2002, Aug. 20-23, 2002, Lugano, Switzerland, pp. 73~74.

(4) B.-K. Lee, D.S. Kim, T.H. Kwon and S.S. Lee, "Replication of Microlens Arrays by Injection Molding", HARMST (High Aspect Ratio Micro-Structure Technology) 2003, submitted.